

# Learning Geometric Invariant Features for Classification of Vector Polygons with Graph Message-passing Neural Network

Zexian Huang<sup>1\*</sup>, Kouros Khoshelham<sup>1†</sup> and Martin Tomko<sup>1†</sup>

<sup>1</sup>Department of Infrastructure Engineering, The University of Melbourne, Grattan Street, Melbourne, 3010, Victoria, Australia.

\*Corresponding author(s). E-mail(s): [zexianh@student.unimelb.edu.au](mailto:zexianh@student.unimelb.edu.au);

Contributing authors: [k.khoshelham@unimelb.edu.au](mailto:k.khoshelham@unimelb.edu.au);

[tomkom@unimelb.edu.au](mailto:tomkom@unimelb.edu.au);

<sup>†</sup>These authors contributed equally to this work.

## Abstract

Geometric shape classification of vector polygons remains a non-trivial learning task in spatial analysis. Previous studies mainly focus on devising deep learning approaches for representation learning of rasterized vector polygons, whereas the study of discrete representations of polygons and subsequent deep learning approaches have not been fully investigated. In this study, we investigate a graph representation of vector polygons and propose a novel graph message-passing neural network (PolyMP) to learn the geometric-invariant features for shape classification of polygons. Through extensive experiments, we show that the graph representation of polygons combined with a permutation-invariant graph message-passing neural network achieves highly robust performances on benchmark datasets (i.e., synthetic glyph and real-world building footprint datasets) as compared to baseline methods. We demonstrate that the proposed graph-based PolyMP network enables the learning of expressive geometric features invariant to geometric transformations of polygons (i.e., translation, rotation, scaling and shearing) and is robust to trivial vertex removals of polygons. We further show the strong generalizability of PolyMP, which enables generalizing the learned geometric features from the synthetic glyph polygons to the real-world building footprints.

**Keywords:** Spatial Vector Polygons; Geometric Shape Classification; Transformation Invariance; Permutation Invariance; Deep Neural Networks

# 1 Introduction

Geometric shape classification of spatial objects is a non-trivial task in spatial analysis. The recognition of spatial objects assisted by automated shape classification is a major enabler of data intensive tasks, including cartographic generalisation, building pattern recognition, archaeological feature analysis, and road geometry identification [1–3].

One of the main challenges in geometric shape classification is the identification of object footprints (i.e., outlines) in the geographic context. A key requirement is the classification of objects invariant to geometric transformations including rotation, scaling, and shearing. The human visual system relies on the Gestalt properties of perceived objects [4, 5] during the classification of shapes. A key property of Gestalt is the invariance to geometric transformations, assuring that geometric shapes are recognized regardless of geometric transformations. In contrast to the human visual perception capabilities, deep learning architectures have been designed and shown to be mainly translation-invariant (e.g., Convolution Neural Networks, CNN) or permutation-invariant (e.g., Graph Neural Networks, GNN) on classification tasks. The ability to reflect Gestalt principles through transformation invariances thus present a strong motivation for an inductive bias in the design of learning-based models for geometric shape recognition of spatial objects.

Spatial objects are often conveniently represented as vector polygons, a data representation thus far neglected in deep learning research. Learning geometric-invariant features from vector polygons has the following requirements: (1) a generic data representation that encodes geometric features of polygons without information loss; and (2) a learning model built on this input data representation that enables learning latent geometric-invariant features robust to geometric transformations. Existing geospatial applications (i.e., shape coding and retrieval [6], building pattern recognition [1, 2] and building grouping [7]) utilizing polygonal geometries motivate us to systemically study geometry encoding methods in conjunction with appropriate and robust learning architectures that enable learning transformation invariant features of spatial polygon geometries.

Veer et al. [2] proposed VeerCNN, a deep convolution model to learn convolutional features on fixed-size 1D vertex sequences of polygon vertices for building attribute recognition. The architectural limitations of CNNs attributable to shared-weights convolutional kernels followed by non-linear activation and fixed-size pooling layers (e.g., *mean*, *sum* or *max*) only enable learning intermediate hierarchical features invariant to translation, with poor handling of rotation, scaling and shearing. Mai et al. [8] noted that CNN models learning on 1D sequences are also sensitive to (1) permutations of the feed-in order of polygon vertices (i.e., sensitive to *loop origin invariance*); and (2) the impact of trivial vertices on the exterior and interiors of polygons, defined by Mai et al. [8] as “[vertices] . . . where the addition or removal of the vertex have no effect on the geometric shape and topological properties of the outlines of the polygons”. In this study, we treat the addition or removal of trivial vertices of polygons as changes that do not alter the semantic information of the shape (captured by the human-assigned label), thus closely reflecting the relationship with the Gestalt principles.

Learning models tailored for discrete (i.e., not grid-like), permutation invariant data representations are predicated on data domains where entries hold no explicit

neighborhood information (e.g., point sets [9–12]). Polygons can then be encoded into point sets of vertices on the exterior and interior rings of the polygons with arbitrary ordering. In contrast to the 1D sequence encoding of polygons, point set encoding assumes input data to have varying input sizes and feed-in order. Models learning on point sets are designed to map input points with permuted order to task-specific outputs (i.e., *permutation invariance* [13]). Here, we argue that such point set representations do not sufficiently capture the connectivity information between vertices of polygons, leading to information loss and performance degradation in geometric shape classification.

Graph data structures present a suitable data encoding for polygons. Recent studies [6, 14, 15] convert vector polygons into un-directed graphs where the vertices on the exteriors and interiors of polygons are captured as graph nodes linked by un-directed graph edges. Compared to fixed-size 1D sequences and varying-size point-set encoding of polygons, graph encoding effectively encapsulates both the geometric and connectivity information of the vertices along the exterior and interior linear rings defining the polygons. Graph-based representations also enable the feed-in order of polygon vertices to be independent of the model outcomes, while the connectivity (topology) between parts of polygon representations remains invariant to geometric transformations.

Graph convolutional autoencoders (GCAE) [6] extend graph convolution neural networks [16] by learning spectral convolution embeddings from polygon graphs and demonstrate the effectiveness of latent embedding. Bronstein et al. [13] discussed that the graph convolution layers aggregate node features from neighboring nodes with constant weights, largely limited by the topological structure of the input graphs. In vector polygons vertices on the linear rings have constant neighbours (i.e., left and right neighbour vertices on linear rings), leading to a reduction in the expressivity of graph convolution features learned from polygon graphs. In this study, we propose to leverage graph message-passing mechanisms [17] in graph-based learning models to learn highly expressive and robust latent features of polygons.

Our hypothesis is that graph representations of polygons enable the learning of robust latent features of polygons invariant to geometric transformations (i.e., rotation, scaling and shearing) when combined with graph message-passing models, thus supporting generalizability on data with domain shifts.

If the hypothesis holds, we suggest that the downstream tasks performed on the learned features of vector polygons lead to robust performance on shapes with varying amounts of trivial vertices. We present the results of a series of experiments designed to evaluate model robustness on polygons altered by geometric transformations, and investigate the generalizability of the findings on combinations of polygon representations and model architectures (permutation-invariant vs. translation-invariant models) for the classification of vector polygons with and without holes (inner linear rings).

After a literature review of related literature (Section 2) we present a synthetic dataset of polygonal shapes of high shape variability with known, robust human labels, based on latin alphabet character glyphs (Section 3.1.1). Despite a broad range of shape variations between fonts (in particular with respect to trivial vertices), characters must maintain strong recognisability attributable to the shapes’ Gestalt. We then

experimentally benchmark the performance of learning models operating on three distinct data representations (1D sequence, set and graph) and varying amounts of geometric transformations (i.e., rotation, scaling and shearing). Our results (Section 4) document the models’ robustness to geometric transformations by benchmarking their performance on the synthetic glyph dataset. Building on these results, we further evaluate the generalizability of the models on a real-world building footprint dataset collected from the Open Street Map (OSM) [6].

Our main contributions are:

1. a thorough investigation of the impact of distinct combinations of graph representation of polygons and message-passing learning architectures for the learning of geometric features robust to geometric transformations of shapes and removals of trivial vertices, grounded in a theoretically grounded set of desiderata;
2. the contribution of an open synthetic dataset of vector polygon shapes based on glyphs, enabling the benchmarking of geometric learning models; and
3. the experimental demonstration that graph representations of vector polygons in conjunction with message-passing neural networks achieve the most robust performance and generalization to real-world shape datasets.

## 2 Background

### 2.1 Machine Learning with Vector Geometries

In a straightforward extension of computer vision approaches devised for image classification, current research on polygonal shape classification typically learns salient geometric features of shapes based on rasterized 2D vector geometries and traditional deep CNN architectures [18, 19].

The geospatial community has adopted these approaches for a variety of remote sensing tasks, including vector shape generation. The Microsoft open building footprints dataset [20] was generated by segmenting and subsequently vectorizing building polygons based on satellite and aerial imagery using deep semantic segmentation networks [21].

Such expertise in image classification naturally influenced approaches to learning tasks on vector shapes. Xu et al. [22] trained a deep convolution autoencoder to assess the quality of geographic information of rasterized building footprints collected from OpenStreetMap (OSM) [23]. Veer et al. [2] evaluated the classification performance of deep neural networks on spatial vector geometries with geometry vertices encoded as 1D sequences directly feed into deep learning models. While this shows the ability of CNNs and RNNs to achieve performances comparable to machine learning methods with hand-crafted features, these approaches neglect the desirable property of learning transformation invariant features of shapes.

Beyond the geospatial community, the typography and computer graphics communities also significantly handle vector shapes. Lopes et al. [24] developed a generative model with convolution layers as encoders, to generate vector text glyphs. Yet, this model is optimized to learn only scale-invariant features of font styles. Mino and Spanakis [25] and Sage et al. [26] generated vector icons and logos from rasterized

images using deep generative autoencoders proposed by Radford et al. [27] and Odena et al. [28]. Furthermore, Ha and Eck [29] proposed a recurrent neural network (RNN), *sketch-rnn*, to generate stroke-based vector drawings of common objects, while later Carlier et al. [30] introduced a hierarchical generative network (DeepSVG) which uses Transformer blocks [31] as the encoder and decoder of a backbone architecture for scalable vector graphics (SVG) generation.

## 2.2 Vector Geometry as Discrete Data Representation

Recently, the progress of graph representation learning [16, 32–34], enabled studies re-formalized learning tasks of vector polygons as graph or set representation learning problems. Previous work by Yan et al. [1] investigated the building pattern classification problem utilizing graph convolution networks. They processed buildings into building clusters, based on geometric patterns of individual buildings. They discovered the relational representations between buildings in graphs built using clusters based on Delaunay triangulation and Minimum Spanning Tree. They then trained a graph convolution model [16] for a binary classification of regular and irregular building clusters. Similarly, Bei et al. [15] devised a spatial adaptive model that makes use of graph encoding, but applied to entire building clusters (i.e., buildings as graph nodes) and applied a graph convolution neural network [16] for group pattern recognition (i.e., inner-state, edge-state and free state building patterns).

Most recently, Yan et al. [6] presented a graph convolutional autoencoder, based on the graph convolution model [16], to analyze the shape of building polygons. Different from previous works, they proposed to represent building polygons as graphs with the vertices of boundary geometries of buildings as graph nodes and their neighbour vertices as description features. However, this method did not consider the relational structures between connected vertices in graphs. Hence, their experiments on building shape coding and empirical results of building shape similarity measurement suggest that the proposed method is sensitive to rotation of building polygons.

Liu et al. [35] proposed a deep point convolutional network (DPCN), a modification of a DGCNN [36], to recognize the geometric shapes of buildings in map space, with the convolution operator **TriangleConv**. Their method operates on the coordinates of vertices of the exterior boundaries of building polygons and the convolution operator **TriangleConv** extracts local geometric features from triangle features, where triangle features are given by  $f_{\text{TriangleConv}}(x_{i-1}, x_i, x_{i+1}) = \{(x_i - x_{i-1}), (x_i - x_{i+1}), (x_{i-1} - x_{i+1})\}$ , and  $(x_{i-1}, x_i, x_{i+1})$  are adjacent coordinate features of a building polygon. This method, trained and evaluated on a building footprint dataset [6], achieves fair classification performances (i.e., accuracy) on geometric shapes of buildings. However, their method requires a pre-definition of local triangles constructed by the graph nodes and adjacency points, and attempts to aggregate the local triangle features (i.e., angles and areas) for updating node features. We argue that learning additional local triangle features of polygons repeatedly is redundant and increase computing overhead in model training, as pointed out by Taylor et al. [37]. Further, they do not evaluate the robustness and generalizability of permutation-invariant data representations and learning architectures to geometric transformations of spatial geometries.

Mai et al. [8] recently proposed a general-purpose polygon encoding model for single and multi-part polygonal geometries. Their polygon encoding method, ResNet1D is a 1D CNN-based polygon encoder that captures local geometric features of spatial polygons and is deemed suitable for shape classification. ResNet1D encodes a polygon coordinate vertex  $i$  as relative offset vectors from  $k$  neighbouring vertices:  $\{x_i, x_{i-1} - x_i, x_{i+1} - x_i, \dots, x_{i+k} - x_i, x_{i-k} - x_i\}$ . They contrast this encoding with a Non-Uniform Fourier Transformation (NUFT) method NUFTspec, based on the shape spectral domain. The NUFTspec aggregates global features of polygons as a NUFT representation and is a better encoding method for geometry topological relation predictions. Their work is thus parallel to our study. Here, we focus on the ability to support specific transformation invariant properties of combinations of learning architectures (permutation-variant CNN, set-based, graph-based and attention-based permutation-invariant models) and data representations (1D grid, set, graph and complete graph).

While some of the above studies leverage graph representations and local geometric encoding of vector polygons and state-of-art graph representation learning models to solve tasks on vector shapes, they do not yet provide a grounded, principled justification for graph-based learning methods on vector polygons. We attempt to fill this gap here by providing experimental results grounded in a sound theoretical motivation, and demonstrate why discrete data representations in combination with permutation-invariant learning models provide desired robustness to vector shape learning tasks.

### 2.3 Graph Representation of Polygon

Polygons are point sets connected by lines, constituting a collection of clock-wise or counter clock-wise linear rings [38]. According to the Gestalt principles of invariance, the compact embedding of linear rings should ideally be invariant to geometric transformations (rotation, scale and shear). We define a graph  $\mathcal{G} = (X, E)$ , where  $X$  is a node matrix that contains the point coordinates of geometry vertices and  $E$  is an edge matrix that captures the connectivity of these vertices along the linear rings (boundaries of the outside and of any holes of polygons), hence encoding the node connectivity of the graph. The binary adjacency value  $a_{ij} = 1 \in A$  is used to indicate the connectivity between nodes  $i$  and  $j$ , with  $A$  being a square adjacency matrix.

### 2.4 Graph Representation Learning

Graph representation learning model leverages the property of data permutations and learns a whole graph embedding  $\mathcal{G}^*$  from the input graph  $\mathcal{G}$  with differentiable permutation-invariant function  $\mathcal{F}$ . The learned embedding  $\mathcal{G}^*$  can be applied to graph-wise and node-wise classifications, or even edge predictions.

By representing polygon linear rings as graphs, we can define a differentiable permutation-invariant function  $\mathcal{F}$ , which takes the graph representations as inputs and returns a corresponding compact graph embedding  $\mathcal{F}(\mathcal{G}; \theta) := \mathcal{F}(X, A; \theta) \rightarrow \mathcal{G}^* \in \mathcal{R}$ .

Considering a permutation matrix  $\mathcal{P}$  operating on graph  $\mathcal{G}$ , the permutation matrix  $\mathcal{P}$  alters the order of node feature matrix  $X$  in  $\mathcal{G}$  along with the adjacency matrix  $A$ ,

producing a perturbed graph  $\mathcal{G}' = (PX, PAP^\top) = (X', A')$ . The ideal permutation-invariant function  $\mathcal{F}$  should satisfy  $\mathcal{F}(X', A'; \theta) = \mathcal{F}(X, A; \theta)$ . We relate the idea of permutation matrix  $\mathcal{P}$  to the aforementioned geometric transformations.

In the view of invariant feature learning, the permutation invariance of  $\mathcal{F}$  outputs are guaranteed through the local aggregations of node features of  $x \in X$  and the linear transformations of aggregated node features:

$$\mathcal{F}(X; \theta) = \rho\left(\sum_{x \in X} \phi(x, \theta)\right).$$

The local differentiable function  $\phi$  linearly transforms each node feature individually  $x$  to latent space and the aggregation function sums over latent node features<sup>1</sup>, and  $\rho$  is a global differentiable function applied on the summed node features followed by a non-linear activation function. In this simple setting, the outputs of  $\mathcal{F}$  are invariant to the permutation of node features since the aggregation sum returns the same outputs for any input permutation:  $Aggr_{sum}(x_1, x_2, \dots, x_n) = Aggr_{sum}(x_n, \dots, x_2, x_1)$ .

This learning setting [9] makes a simple assumption on the permutations acting on input data, which can affect only individual node features without taking into account the connectivity within data (i.e., boundaries of polygon geometries). Graph convolution neural networks (GCN) by Kipf and Welling [16] learn convolutional features of node matrix  $X$  with the normalized graph Laplacian matrix  $\hat{A} = \tilde{D}^{-1/2} \tilde{A} \tilde{D}^{-1/2}$ , where  $\tilde{A} = A + I$  is the adjacency matrix with a identity matrix (i.e., self-connections of nodes), and  $\tilde{D}$  is the diagonal degree matrix. Intuitively, the graph Laplacian matrix describes the divergence of energy flowing from one place (source nodes) to another (target nodes) in a graph. Linking this back to the linear rings of polygons and graph representation, the graph Laplacian conceptually shows similar energy divergence for nodes on the same rings (i.e., polygons with holes) and for nodes that are close to each other (i.e., polygons without holes).

Thus, GCN can learn graph Laplacian embedding of node feature with a differentiable neural network layer as follows:

$$\begin{aligned} \mathcal{F}_{conv}(X, A; \theta) &= \tilde{D}^{-1/2} \tilde{A} \tilde{D}^{-1/2} X \theta \\ &= \hat{A} X \theta. \end{aligned} \tag{1}$$

We can express Eq.1 from a vector-wise view:

$$f(x_i; a_{ij}, \theta) = \sum_{\substack{a_{ij} \in A, \\ x \in X}} \phi(x_i, x'_j, \theta), \text{ where } x'_j = \frac{\tilde{a}_{ij}}{\sqrt{\tilde{d}_i \times \tilde{d}_j}} x_j, \tag{2}$$

$\frac{\tilde{a}_{ij}}{\sqrt{\tilde{d}_i \times \tilde{d}_j}}$  corresponds to the edge weight between nodes  $x_i$  and  $x_j$  in the normalized graph Laplacian matrix  $\hat{A}$ . From Eq.2, the latent feature of target node  $x_i$  depends on the relation with its neighbour node  $x_j$  and constant edge weight  $\frac{\tilde{a}_{ij}}{\sqrt{\tilde{d}_i \times \tilde{d}_j}}$ . However,

---

<sup>1</sup>The basic aggregation in this setting can also be averaging or max pooling.

the constant edge weight between nodes  $x_i$  and  $x_j$  largely limits the expressivity of latent node features of polygonal graph since every node has a constant node degree ( $d = 2$ ).

As discussed in Yan et al. [6], graph autoencoders GCAE based on GCN are sensitive to orientation and rotation of polygons, and therefore current graph-based learning methods are not optimized for geospatial settings with polygonal geometries of arbitrary orientation, or conversely, arbitrary observer orientation. Here we propose to leverage the message-passing mechanism [17, 39] with the permutation-invariant function  $\mathcal{F}$  to learn expressive and robust latent features of polygons.

## 2.5 Message-passing Neural Network

The principle of the message-passing mechanism is the aggregation of neighbour node features in graphs based on the “message” computed between the source and target nodes. We define the message-passing function operating on a single node as:

$$h_i = \phi(x_i, msg(x_i, x_j), \theta), \quad (3)$$

where  $\{x_i, x_j\} \in A = 1$  and  $msg(\cdot)$  is a message function with the source and target nodes as inputs. From Eq.3, the node feature of  $x_i$  is updated with the computed message  $(x_i, x_j)$ , and together linearly transformed into latent space, producing the latent feature  $h_i \in \mathcal{H}$ .

Eq. 4 present the message-passing neural network in vector view as follow:

$$\mathcal{F}_{msg}(X, A; \theta) = \rho_{\theta}(readout(h_i | h_i \in \mathcal{H})). \quad (4)$$

A global readout function (i.e., mean or max pooling) summarizes the latent node-wise features ( $\mathcal{H}$ ) and computes a global graph embedding for the input graph by non-linearly transforming the pooled feature.

Hence, we propose a **M**essage-**p**assing neural network for **P**olygon geometries, PolyMP, as shown in Fig. 1. The PolyMP considers the point coordinates of polygons as input node features and the exterior connectivity of polygons as input edges. The message-passing layers of PolyMP then compute the “message” for each node according to the graph adjacency. Following existing works on point clouds [11, 36] and polygons Liu et al. [35], we compute the message of relative positions of two connected nodes:  $msg(x_i, x_j) = |x_j - x_i|$ , which enable aggregating the local geometric features of polygons for updating node features. After message-passing layers, a global pooling layer is applied over the polygons with aggregated node features to generate a whole graph embedding, which is then used for the downstream shape classification of polygons.



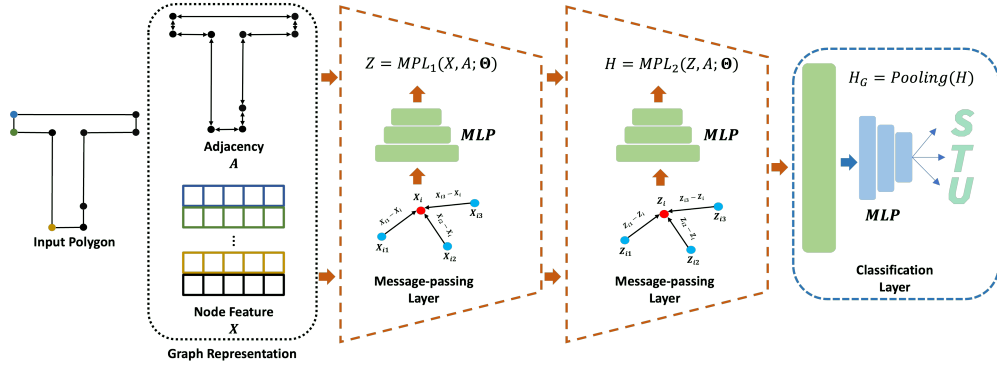


**Fig. 1** Model architecture of PolyMP. PolyMP consists of two message-passing layer and a classification layer (Multi-layer perceptron).

## 3 Experiment

### 3.1 Datasets

#### 3.1.1 Glyph Dataset

We introduce a synthetic dataset of highly variable geometric shapes for benchmarking the classification performance of learning models on vector polygons. The dataset consists of 26 Latin alphabet character glyph geometries (here also equal to semantic classes **A** to **Z**) of fonts gathered from an online source [40]. An equivalent approach to construct a rich dataset of geometric shapes has been used to test algorithms in computational geometry before [41].

We extract the boundaries of glyphs ( i.e., contour lines, as called in typography) for 1,413 sans serif and 1,002 serif fonts, to produce 2D simple polygon geometries compliant with OpenGeospatialConsortium [38]. Serif and sans serif fonts are the two main typographic font families. Serif glyphs have salient decorative strokes ending the main character strokes increasing legibility of body text, whereas sans serif glyphs have clean strokes suitable e.g., for the display of headers. Importantly, these minor variations do not alter the Gestalt of the shapes (as proven by reader’s ability to consistently read the symbols). Thus, the labels assigned to the symbols are stable and robust. We encode each polygon geometry into a fixed-size feature matrix  $\in R^{n \times 3}$  where each feature vector  $\in R^3$  includes the 2D coordinates of vertices  $(x, y)$  as geometric feature and a binary feature  $(0, 1)$  to indicate the positions of 2D coordinates, whether on outer rings or holes of polygons. Examples of glyph geometry are displayed in Figure 2.

#### 3.1.2 OSM Dataset

Latin alphabet glyph geometries share geometric similarity with building footprints. We use a building geometry dataset designed to test the generalizability of learning



**Fig. 2** Glyph dataset samples. Left to right columns: A-shape to J-shape glyphs.

models on spatial objects proposed by Yan et al. [6]. The dataset contains 10,000 real-world building footprints extracted from OSM [23], labelled by 10 categories based on a template matching to letters [42]. The building footprints are randomly rotated and reflected from the original canonical samples (Figure 3). This is currently the most comprehensive real-world dataset of vector geometries with purely shape-based labels (as opposed to, e.g., building use, which should not be used for shape classification). We note that the assignment of labels in this dataset is somewhat subjective and likely less robust than in the glyph-based dataset. Note, in particular, that shape reflection is problematic for label stability, e.g., for asymmetric letters ( $R$ ), or mirror shapes of distinct labels ( $S, Z$ ).

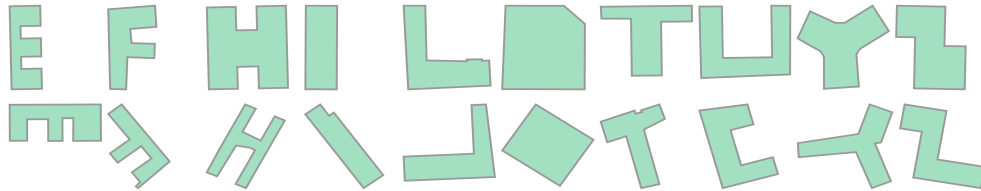


**Fig. 3** OSM dataset samples. Top row: building geometries of standard shapes. Bottom row: geometric transformation counterparts. Left to right columns: E, F, H, I, L, O, T, U, Y and Z-shape buildings. [6]

### 3.1.3 Pre-processing

#### *Label-preserving transformations*

To examine the invariances of geometric transformations of polygon representations and corresponding learning models with respects to data transformations, we consider four training datasets under data transformations, each consisting of 20%, 40%, 60% and 80% of glyph polygons that have undergone label-preserving geometric transformations. The details of transformations are presented in Table 1. The original and transformed data samples are visualised in Fig. 4. We thus obtain five training datasets, including the original dataset: dataset 0%, 20%, 40%, 60% and 80% for the experiment. The test set consists of data randomly sampled from the five datasets.

#### *Polygon Simplifications*

To test the invariances to trivial vertices of polygon, we apply the Douglas–Peucker algorithm [43] (tolerance = 1.0) on the original size of glyph polygon (in the order of

**Table 1** Label-preserving transformations applied to samples of Glyph dataset maintains the semantic information (label) of original polygons (i.e., 180 degrees rotation of letter M alter its semantic label, converting to letter W).

Transformation	Operation
Rotation	Rotate data around its centroid by a random angle $\in [-75^\circ, 75^\circ]$ .
Scaling	Scale data by random distinct factors $\in [0.1, 2]$ on the $x$ and $y$ axes.
Shearing	Shear data in a random angle $\in [-45^\circ, 45^\circ]$ on the $x$ and $y$ axes.

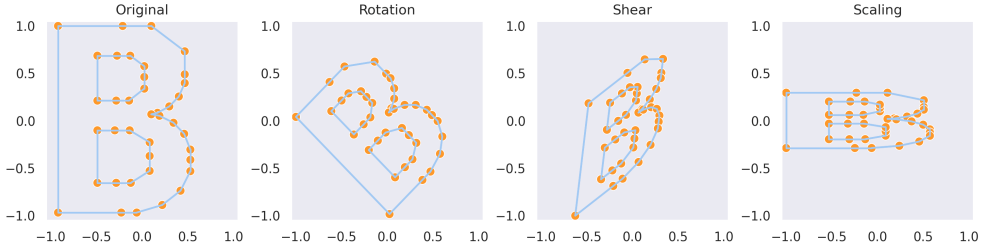


**Fig. 4** Data samples of Glyph dataset under label-preserving transformations.

$50 \times 50$  units) to generate simplified samples for glyph dataset. The resulting polygon linestrings are defined by fewer vertices (in particular, excluding all co-linear or close to co-linear vertices). Notice that the simplification occurs before the normalisation to the range of  $(-1,1)$  and any augmentation of polygons, ensuring that the simplified geometries preserve the topology and essence of the shape of the original glyph (see Fig. 5).

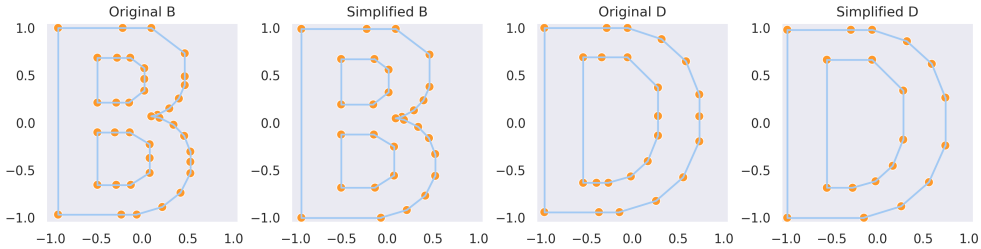


**Fig. 5** Visualisation of original and simplified polygon examples generated with Douglas–Peucker algorithm [43]. The simplified polygons, compared to original polygons, contain a subset of the vertices that defined the original curve.

### 3.2 Training Configuration

We evaluate the performances of learning models from previous studies, in particular: the VeerCNN in Veer et al. [2], based on 1D sequences converted from polygons as

inputs; the DeepSet from Zaheer et al. [9] and SetTransformer Lee et al. [12], based on polygon vertices as input point clouds; and the GCAE in Yan et al. [6], representing polygons as input graphs. We then compare their performances with the proposed message-passing model for polygons (PolyMP).

The model configurations used in our experiments are in Table 2. Correspondingly, we depict the data representations of polygons and baseline models in Figure 6. The proposed PolyMP is demonstrated in Figure 1. For experimental control, every model tested was constrained to a comparable model depth and latent space of feature embedding.

For model training on Glyph dataset and fine-tuning on OSM dataset, we compute the cross entropy loss [44] to determine training gradients for fast training convergence and good model generalizability. We use the Adam optimization [45] with an initial learning rate of 0.01. For better model generalization, we adopt a learning rate decay strategy that reduces the learning rate by a factor of 10 once the model training reaches a performance plateau over 25 epochs. An early-stopping mechanism halts the training once the loss ceases to decrease for 50 epochs, to mitigate overfitting. We set the batch size to 64 and the total training epochs to 100. Thus, importantly, the models here are not designed to individually outperform current state-of-the-art for each architecture, but to maintain comparability across architectures and to enable evaluation of the effects of data representations on the results.

**Table 2** Model configuration. Each model is configured to have the same number of convolution layers and dimensions of latent embedding, to keep the model size (i.e., number of training parameters) comparable.

Model	Conv. depth	Latent dim.	#Param.	Pooling
VeerCNN [2]	2	{2, 32, 64}	13,853	Global avg.
DeepSet [9]	2	{2, 64, 64}	11,837	Global avg.
SetTransformer [12]	2	{2, 64, 64}	113,531	Attention
GCAE [6]	2	{2, 64, 64}	7,613	Global avg.
PolyMP (Ours)	2	{2, 64, 64}	11,837	Global avg.

## 4 Result

We report model performances for all experiments as the overall accuracy (O.A.), calculated as the ratio of true positives over the total number of samples.

### 4.1 Results on Glyph Dataset

Table 3 and 4 demonstrates the model performances testing on Glyph dataset and the simplified polygons, respectively.

At 0% transformation ratio in Table 3, we observe that the PolyMP achieves 99.41%, 42.91% and 80.03% acc. on the original, rotated and scaled test samples, whereas VeerCNN achieves 59.07% acc. on sheared samples. While deepset, set transformer and GCAE maintain comparable performances (94.62%, 65.01%; and 96.25%,

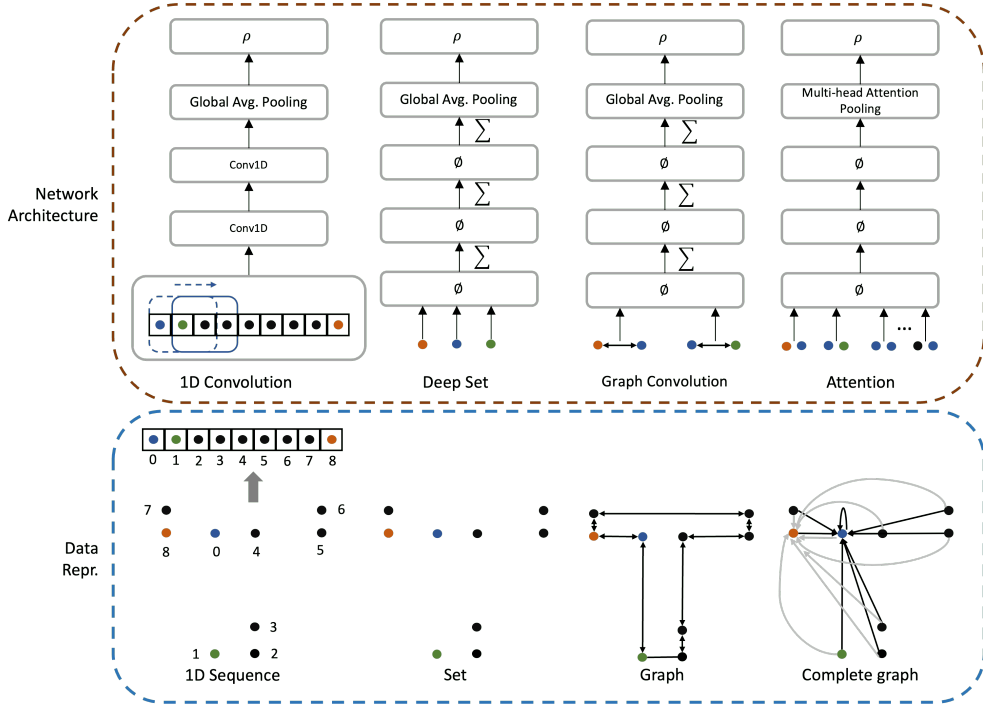


**Fig. 6** Data representations of polygons (as 1D sequence, Point Set, Graph and Complete Graph) and the corresponding learning models (Baselines: VeerCNN, DeepSet, GCAE and SetTransformer).

67.91%; and 95.16%, 64.54%, respectively) on original and scaled test samples, the models suffer large performance deterioration, achieving only 23.67%, 26.00% and 25.23%, 27.79% and 31.38% and 38.84% test acc. on rotated and sheared samples, respectively. From the overall accuracy, the VeerCNN outperforms the PolyPM by a slight margin (69.43% and 69.01%).

At 20% transformation ratio, the PolyMP improves model test acc. on rotated, scaled and sheared samples rapidly, achieving 83.17% (+40.26%), 91.29% (+11.26%) and 86.86% (+33.54%) respectively. In overall acc., the PolyMP achieves 90.12% O.A. (+21.11%) and outperforms VeerCNN. In comparison, the other models can not match with PolyMP and achieve comparable performances from increasing data diversity of training set.

At 40% and 60% transformation ratio, we notice that the accuracy improvements gained from increasing the ratio of geometric transformed samples in training set have converged. In this case, the PolyMP maintains its leading performances among models (91.91% and 93.06% O.A.), and VeerCNN (83.30% and 84.88% O.A.), deepset (80.12% and 81.49% O.A.), set transformer (80.33% and 81.94% O.A.) and GCAE (72.72% and 75.50% O.A.) fall behind.

At 80% transformation ratio, the PolyMP achieves the optimal test performances at rotated and sheared samples, giving 90.35% and 91.52% test accuracy. This empirical results suggest that compared to the sequence encoding of polygons and CNN as well as the set representation and set-based learning models, the graph representation together with message-passing neural network (i.e., PolyMP) are robust to the permutations of feed-in order of polygon vertices, which occurs in geometric transmutations of polygons, in particular rotation and shearing.

From a different perspective, the ratio of original samples is decreasing in the training set progressively from the 0% to 80% transformation ratios datasets. The PolyMP only encounters 1.46% test performance deterioration along this progression (99.41% to 97.95% acc.), while the VeerCNN (-4.13% acc.), deepset (-3.96% acc.), set transformer (-5.08% acc.) and GCAE (-5.58% acc.) suffer larger performance drops on the test accuracy of original samples.

In Table 4, the test performances of models trained and evaluated on the simplified polygons of Glyph dataset are presented. In this experiment setting, we focus on models’ test performances on simplified polygons containing fewer numbers of vertices, and compare them with the test performances showed in Table 3.

We observe similar test performance trends to those of models evaluated on the simplified polygons. Noticeably, there is a significant performance deterioration in VeerCNN compared with the test performances in Table 3 on simplified polygons. Specifically, at 0% transformation ratio, the test performances of VeerCNN drops from 69.43% O.A. (Table 3) to 66.56% O.A. (Table 4), i.e., a 2.87% performance deterioration. As the data diversity increases, the performance deterioration in VeerCNN increases, too, from 5.2%, progressively through to 5.56% O.A. deterioration respectively from 20% to 80% transformation ratios.

The performance deterioration of VeerCNN strongly indicates that CNN models are not robust to varying the numbers of vertices in polygons. This can be attributed to a number of factors, incl. the data encoding of polygons in VeerCNN as as fixed-length 1D sequences with zero padding. Simplifying polygons and removing trivial vertices from polygons alters the length of 1D sequences, and hence the geometric information of simplified polygons are not only diluted by the zero padding in the 1D sequences, but also by alteration of vertex adjacency explicitly encoded in the 1D sequence.

In comparison, we notice only small performance drops occur in general set-based and graph-based learning models. We credit this to set and graph representation of polygons and the corresponding learning models as both set and graph-based models accept input polygons of varying lengths. In particular, the graph-based message-passing network (i.e., PolyMP) learns salient local node features from connected neighbours in the message-passing function with permutation-invariant pooling operations (i.e., Max-pooling), as shown in E.q. 4. A similar pooling operation is also adopted in set-based learning models [9, 12].

**Table 3** Test performances on Glyph dataset. Transformation ratios 0%, 20%, 40%, 60% and 80% refer to training datasets consisting of 0%, 20%, 40%, 60% and 80% geometric transformed samples. Glyph-O, Glyph-R, Glyph-SC and Glyph-SH Acc. indicate the classification accuracy of models tested on original, rotated, scaled and sheared data. Overall accuracy is reported as Glyph O.A..

Trans. Ratio	Model	Glyph-O Acc.	Glyph-R Acc.	Glyph-SC Acc.	Glyph-SH Acc.	Glyph O.A.
0%	VeerCNN	97.64	41.51	79.15	<b>59.07</b>	<b>69.43</b>
	DeepSet	94.62	23.67	65.01	26.00	52.56
	SetTransformer	96.25	25.23	67.91	27.79	54.42
	GCAE	95.16	31.38	64.54	38.84	57.83
	PolyMP	<b>99.41</b>	<b>42.91</b>	<b>80.03</b>	53.32	69.01
20%	VeerCNN	95.12	67.63	83.53	77.78	81.05
	DeepSet	93.88	67.95	77.31	64.72	76.25
	SetTransformer	93.87	71.72	82.43	72.56	80.18
	GCAE	93.31	47.31	71.47	57.11	67.61
	PolyMP	<b>98.92</b>	<b>83.17</b>	<b>91.29</b>	<b>86.86</b>	<b>90.12</b>
40%	VeerCNN	94.75	73.26	84.77	80.29	83.30
	DeepSet	92.57	74.24	79.24	72.08	80.12
	SetTransformer	91.97	72.73	83.25	73.25	80.33
	GCAE	91.70	59.55	74.35	64.42	72.72
	PolyMP	<b>98.48</b>	<b>87.06</b>	<b>92.49</b>	<b>89.25</b>	<b>91.91</b>
60%	VeerCNN	94.50	77.16	85.38	82.36	84.88
	DeepSet	91.72	76.89	81.46	73.97	81.49
	SetTransformer	90.93	77.04	82.39	77.31	81.94
	GCAE	90.46	65.02	76.38	68.78	75.50
	PolyMP	<b>98.30</b>	<b>89.40</b>	<b>93.43</b>	<b>91.11</b>	<b>93.06</b>
80%	VeerCNN	93.51	78.97	85.25	83.17	85.25
	DeepSet	90.66	78.68	82.14	76.55	82.47
	SetTransformer	91.17	79.94	83.69	79.78	83.67
	GCAE	89.58	67.95	77.99	70.55	76.83
	PolyMP	<b>97.95</b>	<b>90.35</b>	<b>93.30</b>	<b>91.52</b>	<b>93.42</b>

## 4.2 Results on OSM Dataset

We fine-tune models pre-trained on the glyph 80% dataset with the OSM dataset, and report the classification test accuracy of fine-tuned models in Table 5 for building footprints with original and normalised coordinates respectively.

PolyMP achieves optimal test performance on normalised footprints with 91.92% O.A. on the OSM dataset, and performs better than all other methods. Both set-based methods (i.e., DeepSet: 95.71% and SetTransformer: 94.99%) and graph-based GCAE (94.79%) achieve comparable performance on OSM-O dataset with building footprints without geometric transformations. Conversely, the convolutional VeerCNN shows lower performance of 90.54%. When testing on OSM-R with randomly rotated and reflected footprints, PolyMP maintains a robust performance of 85.62% and the baseline methods suffer performance deterioration at various levels (VeerCNN:

**Table 4** Test performances on Glyph dataset, consisting of simplified polygons generated by Douglas–Peucker algorithm (tolerant=1.0) with the removal of trivial vertices.

Trans. Ratio	Model	Glyph-O Acc.	Glyph-R Acc.	Glyph-SC Acc.	Glyph-SH Acc.	Glyph O.A.
0%	VeerCNN	94.72	39.65	75.42	<b>56.12</b>	66.56
	DeepSet	94.01	23.75	65.11	25.53	52.30
	SetTransformer	94.57	23.67	65.72	26.61	52.76
	GCAE	94.83	31.64	64.21	39.90	58.08
	PolyMP	<b>98.89</b>	<b>43.71</b>	<b>79.15</b>	52.70	<b>68.63</b>
20%	VeerCNN	90.55	62.58	77.80	72.31	75.85
	DeepSet	93.81	68.26	77.83	64.93	76.47
	SetTransformer	92.31	70.51	80.54	70.65	78.54
	GCAE	92.26	47.29	71.28	57.33	67.39
	PolyMP	<b>97.61</b>	<b>82.45</b>	<b>88.42</b>	<b>84.84</b>	<b>88.22</b>
40%	VeerCNN	89.63	67.82	78.72	74.61	77.73
	DeepSet	92.66	74.81	79.60	71.62	80.46
	SetTransformer	89.86	70.91	80.70	70.97	78.14
	GCAE	91.65	59.30	74.95	64.79	72.94
	PolyMP	<b>97.55</b>	<b>86.14</b>	<b>89.99</b>	<b>87.29</b>	<b>90.21</b>
60%	VeerCNN	89.29	71.91	79.42	77.29	79.50
	DeepSet	91.58	77.44	81.62	73.84	81.57
	SetTransformer	89.70	75.03	80.26	75.53	80.15
	GCAE	90.06	63.61	76.64	68.05	74.79
	PolyMP	<b>97.35</b>	<b>88.73</b>	<b>91.04</b>	<b>89.31</b>	<b>91.47</b>
80%	VeerCNN	88.05	73.89	79.55	77.17	79.69
	DeepSet	91.04	79.21	82.44	76.45	82.67
	SetTransformer	89.99	79.14	82.70	78.60	82.63
	GCAE	88.22	66.55	78.01	70.44	76.06
	PolyMP	<b>97.01</b>	<b>90.19</b>	<b>91.53</b>	<b>90.31</b>	<b>92.22</b>

90.54%  $\rightarrow$  78.51%, DeepSet: 95.71%  $\rightarrow$  84.86%, SetTransformer: 94.99%  $\rightarrow$  83.87%, GCAE: 94.79%  $\rightarrow$  80.19%).

Performances of models fine-tuned on OSM footprints with original spatial coordinates drop for all models except for PolyMP, which maintains a performance of 81.58% O.A.. This robust performance of PolyMP against the translation of spatial coordinates can be accounted for by the message-passing network of PolyMP where the local geometric features of polygons are computed (i.e., the relative positions of polygons  $msg(x_i, x_j) = |x_j - x_i|$ ). This relative positional features reduce the impact of absolute positioning and effectively normalise the spatial coordinates of polygons while preserving the geometric properties of polygons. VeerCNN outperforms DeepSet (24.34% O.A) and CGAE (23.18% O.A) and achieves a test performance of 42.68% O.A. when fine-tuned on the original OSM footprints. We account for VeerCNN’s performance by the built-in translation invariant priors in conventional convolution



neural networks. Similarly, SetTransformer shows comparable performance as VeerCNN (44.72% O.A), which can be attributed to the self-attention features based on the fully connected graph of point sets.

In Fig. 7, we visualise the classification results of PolyMP evaluated on spatial building footprints in OSM-O (Fig. 7 (a)) and OSM-R (Fig. 7 (b)). Predictions indicate that the fine-tuned PolyMP can robustly classify building footprints on a map in varying sizes and geometric shapes based on the geometric invariant features learnt by message-passing networks, taking the graph-based representation of polygons as inputs.

**Table 5** Fine-tune test performances on OSM dataset. OSM-O and OSM-R acc. suggest the the classification accuracy of models tested on original and rotated & reflected samples. Overall accuracy is reported for OSM O.A..

Model	OSM-O Acc.	OSM-R Acc.	OSM O.A.	
VeerCNN	90.54	78.51	84.52	Normalised coordinates $\in (-1, 1)$
DeepSet	95.71	84.86	90.56	
SetTransformer	94.99	83.87	89.42	
GCAE	94.79	80.19	88.02	
PolyMP	<b>98.04</b>	<b>85.62</b>	<b>91.92</b>	
VeerCNN	42.35	43.01	42.68	Original coordinates
DeepSet	24.12	24.08	24.34	
SetTransformer	44.67	44.77	44.72	
GCAE	23.44	23.04	23.18	
PolyMP	<b>89.86</b>	<b>73.56</b>	<b>81.58</b>	

## 5 Discussion

### 5.1 Model Expressivity

For the interpretation of model expressivity with respect to various polygon encodings and learning models, we visualize the feature maps of models tested on original and geometric transformed samples in glyph dataset in Figure 9.

Figs. 9a and 9b depict the salient feature maps and class predictions of four models (Deepset, Set Transformer, GCAE and PolyMP) on geometric transformed samples (sheared and rotated glyph M). In this case, the PolyMP correctly predicts the class label of glyph M, whereas DeepSet, Set Transformer and GCAE have made incorrect predictions on the geometric transformed samples. By comparing the feature maps in Figures 9c and 9d, the PolyMP learns to identify the global structures or the “skeleton” of polygons via non-trivial vertices on the boundary. The message-passing network and local pooling function (i.e., max-pooling) can capture the salient vertices from local neighbours (i.e., non-trivial vertices (dark color) in the clusters of trivial vertices (light color)), which enable a robust embedding of polygons under geometric transformations. Set-based models and GCAE learn sparser geometric features for input polygons,

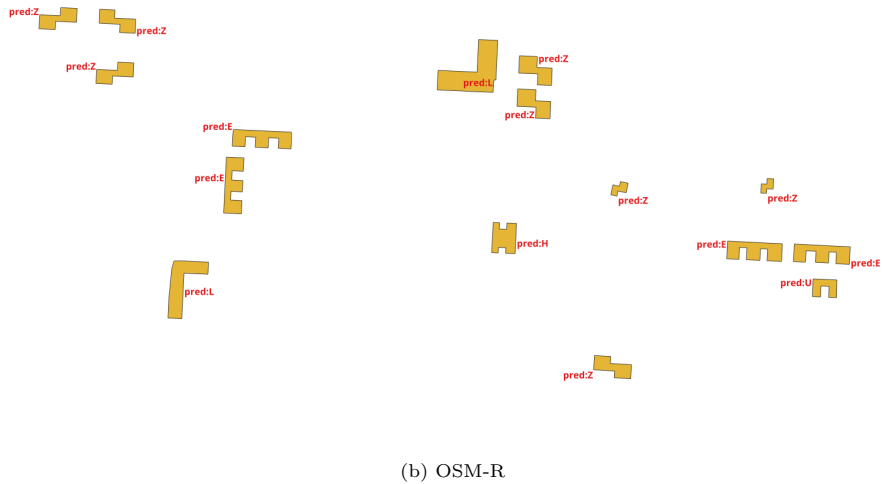
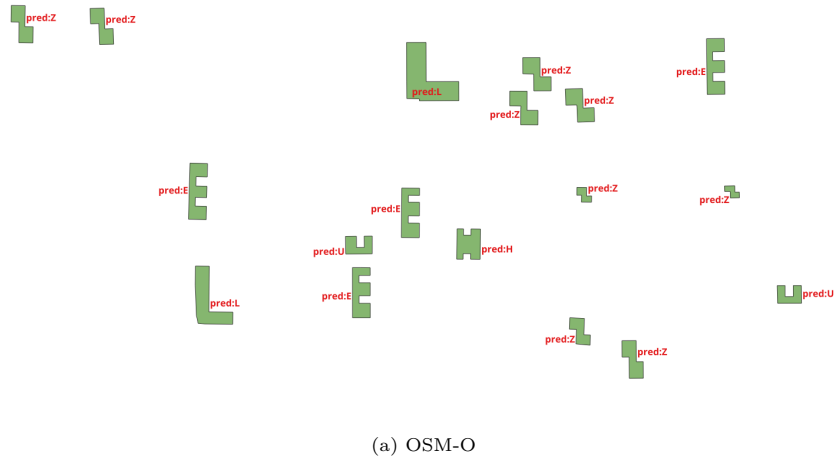
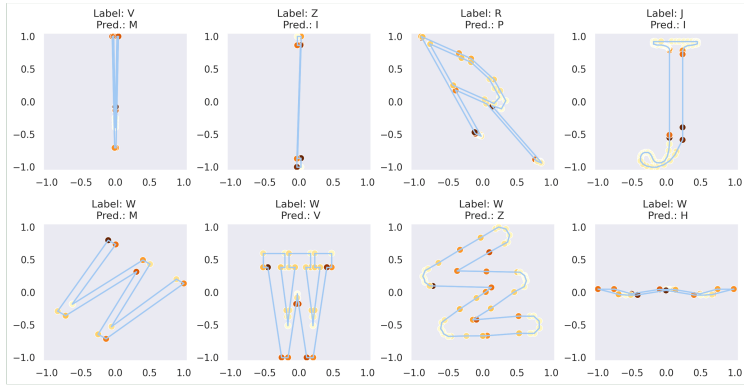


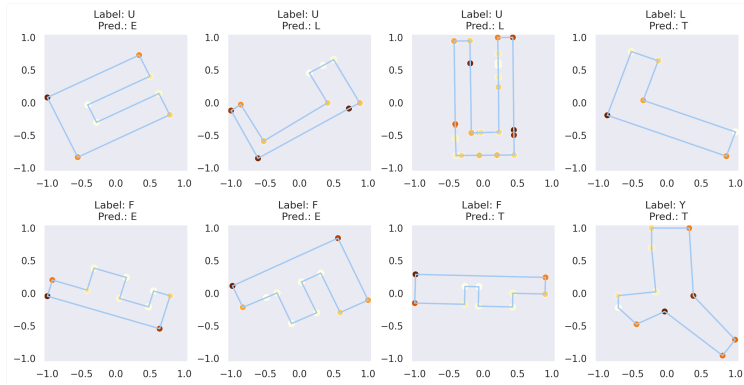
**Fig. 7** Shape classification of building footprints by PolyMP on the selected region in OSM dataset (downtown areas of Shanghai, China [6]). Model predictions are colored in red.

capturing salient features regionally in node clusters and ignoring geometric features of more distant nodes. This can be attributed to the set representation where any relational information between nodes is neglected.

Figures 9e and 9f demonstrate the feature maps on polygons with holes. Both Deepset and Set Transformer only capture geometric features from non-trivial vertices located at the exterior boundary of polygons. While set-based models accept point set encoding of polygons in varying length and the output features are invariant to the



(a) Glyph dataset.



(b) OSM dataset.

**Fig. 8** Failure cases of PolyMP on Glyph and OSM datasets.

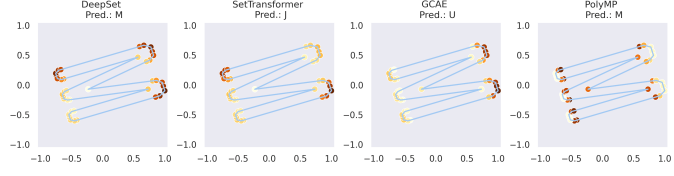
feed-in order of vertices, such methods largely ignore the connectives and interactions between points. Such a learning setting inherently hinders the model’s capability to learn geometric information from polygons with holes. The graph convolution model, GCAE, lacks learning flexibility in learning local geometric features as discussed in the previous sections. On the other hand, PolyMP can capture geometric features from salient points located at the exterior and interiors of polygons. In the message-passing network, the exterior and interior of polygons are considered to be two distinct elements as there is no direct connection between points located at the two boundaries. In other words, the geometric features (i.e., the “message”) are only passed between points that are connected in a connected component of a graph, in this case defined by the linear rings of polygon boundaries.

## 5.2 Limitations

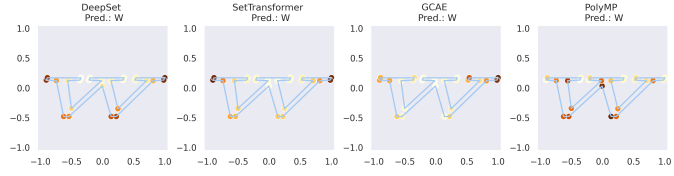
Of course, PolyMP still encounters limitations in terms of misclassification. Fig. 8. demonstrates failures of PolyMP classifications on the Glyph and OSM datasets. On synthetic data, misclassifications occur predominantly on samples where excessive



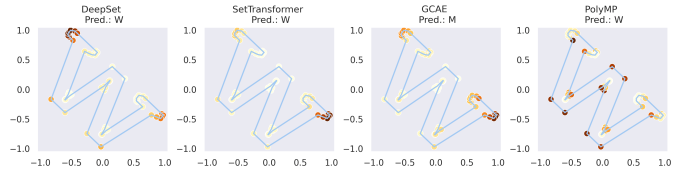
(a) Sheared M glyph.



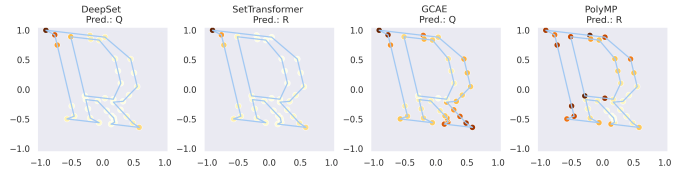
(b) Rotated M glyph.



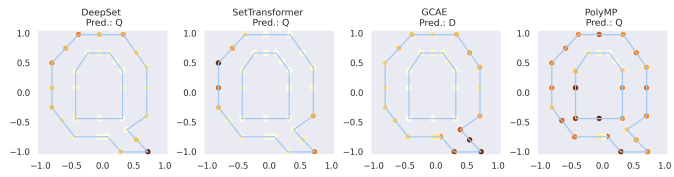
(c) Scaled W glyph.



(d) Rotated W glyph.



(e) Sheared R glyph.



(f) Original Q glyph.

**Fig. 9** Feature maps to visualize salient features learned by individual models to classify input geometries to output categories. The darker the color, the more salient are the features learned. Feature values are normalised  $\in [0, 1]$ .

geometric transformations (e.g., heavy shearing and anisotropic scaling) destroy the gestalt of the shape to the extent it is no longer label preserving (Fig. 8(a): letter V, Z and R). A special case are shapes with different labels dependent on orientation – M and W, where depending on the extent of rotation and shearing, misclassifications occur. For instance in row two of Fig. 8(a), we observe that rotated letters W can be misclassified into letter M, or even Z; heavily sheared W can be misclassified as H and V. Similarly for building polygons (OSM), PolyMP may misclassify polygons sharing similar geometric shapes (E, vs L or U) (Fig. 8).

Considering the characteristics of the two datasets (Sec. 3.1), PolyMP trained Glyph dataset learns locally salient geometric features via message-passing layers from serif glyphs, which contain salient decorative strokes ending. Letters sharing similar geometric shapes are misclassified when the geometric shapes of classified polygons are destroyed by excessive geometric transformations.

## 6 Conclusion

Based on extensive empirical evidence given by the analysis of invariances to geometric transformations, trivial vertices and model generalizability, we demonstrate that discrete, non-grid like data representations in combination with graph-based message-passing neural networks (PolyMP) are optimal for deep learning models on 2D vector geometries. We demonstrate a robust ability to learn shapes of polygonal geometries, and demonstrate the ability to generalize to a real-world building footprint dataset.

We find that a learning model based on graph data representation that explicitly encodes both node and explicit edge structures leads to a robust approach enabling highly accurate feature learning on geometric shapes – conveniently, these structures are readily available from the 2D simple feature representations of geometries implemented in current GIS libraries. Our results indicate that representations play an important part providing a strong inference bias for geometric shape learning, and tasks such as the classification of polygons and boosting model performance. We believe that our approach to learning geometric-invariant features of polygons is not limited to simple geometric shape classification. This approach can benefit suitable geospatial tasks where the geometric-invariant features of polygons matches the learning objectives (i.e., geospatial regression tasks involving spatial relation predictions of polygon map [8]).

We also discuss the limitations of PolyMP through misclassification examples on datasets. Through the failure cases of classification, we observe that the message-passing network for graph data representation of polygons has limited capability of transferring locally salient geometric features from one domain to another. The simple message-passing network has limited control on learning/not learning geometric invariant features as need.

The geometric invariant feature learning of vector geometries is currently an area of intense investigation in spatial deep learning [1, 2, 6, 8, 35]. Unlike in learning based on raster datasets or point clouds, the segmentation problem is partially solved by the explicit encoding of structured vector geometries. Here, we show results that allow us to undertake the classification of spatial geometric shapes efficiently, based on

decisions that can be grounded in theory and are experimentally validated. In future work, we will further examine how richer graph encoding of the structure of geometries, as well as of the relationships between proximal geometries could further boost model performance, or enable the segmentation of complex spatial object arrangements.

## Statements and Declarations

**Data availability.** The data and codes that support the findings of this study are available with the identifier(s) at the private link: <https://figshare.com/s/b781d7724d3220e24c7c>.

**Conflicts of interest.** This paper has been approved by all co-authors. The authors have no competing interests to declare that are relevant to the content of this article.

## References

- [1] Yan, X., Ai, T., Yang, M., Yin, H.: A graph convolutional neural network for classification of building patterns using spatial vector data. *ISPRS journal of photogrammetry and remote sensing* **150**, 259–273 (2019)
- [2] Veer, R.v., Bloem, P., Folmer, E.: Deep learning for classification tasks on geospatial vector polygons. arXiv preprint arXiv:1806.03857 (2018)
- [3] Andrášik, R., Bíl, M.: Efficient road geometry identification from digital vector data. *Journal of Geographical Systems* **18**(3), 249–264 (2016)
- [4] Lehar, S.: *The World in Your Head: A Gestalt View of the Mechanism of Conscious Experience*. Lawrence Erlbaum, Mahwah, N.J. (2003)
- [5] Lehar, S.: Gestalt isomorphism and the primacy of subjective conscious experience: A gestalt bubble model. *Behavioral and Brain Sciences* **26**(4), 375–408 (2003)
- [6] Yan, X., Ai, T., Yang, M., Tong, X.: Graph convolutional autoencoder model for the shape coding and cognition of buildings in maps. *International Journal of Geographical Information Science* **35**(3), 490–512 (2021)
- [7] Yan, X., Ai, T., Yang, M., Tong, X., Liu, Q.: A graph deep learning approach for urban building grouping. *Geocarto International* **37**(10), 2944–2966 (2022)
- [8] Mai, G., Jiang, C., Sun, W., Zhu, R., Xuan, Y., Cai, L., Janowicz, K., Ermon, S., Lao, N.: Towards general-purpose representation learning of polygonal geometries. *GeoInformatica*, 1–52 (2022)
- [9] Zaheer, M., Kottur, S., Ravanbakhsh, S., Póczos, B., Salakhutdinov, R.R., Smola, A.J.: Deep sets. *Advances in neural information processing systems* **30** (2017)

- [10] Qi, C.R., Su, H., Mo, K., Guibas, L.J.: Pointnet: Deep learning on point sets for 3d classification and segmentation. In: Proceedings of the IEEE Conference on Computer Vision and Pattern Recognition, pp. 652–660 (2017)
- [11] Qi, C.R., Yi, L., Su, H., Guibas, L.J.: Pointnet++: Deep hierarchical feature learning on point sets in a metric space. *Advances in neural information processing systems* **30** (2017)
- [12] Lee, J., Lee, Y., Kim, J., Kosiorek, A., Choi, S., Teh, Y.W.: Set transformer: A framework for attention-based permutation-invariant neural networks. In: International Conference on Machine Learning, pp. 3744–3753 (2019). PMLR
- [13] Bronstein, M.M., Bruna, J., Cohen, T., Velicković, P.: Geometric deep learning: Grids, groups, graphs, geodesics, and gauges. *arXiv preprint arXiv:2104.13478* (2021)
- [14] He, X., Zhang, X., Xin, Q.: Recognition of building group patterns in topographic maps based on graph partitioning and random forest. *ISPRS Journal of Photogrammetry and Remote Sensing* **136**, 26–40 (2018)
- [15] Bei, W., Guo, M., Huang, Y.: A spatial adaptive algorithm framework for building pattern recognition using graph convolutional networks. *Sensors* **19**(24), 5518 (2019)
- [16] Kipf, T.N., Welling, M.: Semi-supervised classification with graph convolutional networks. In: International Conference on Learning Representations (ICLR) (2017)
- [17] Gilmer, J., Schoenholz, S.S., Riley, P.F., Vinyals, O., Dahl, G.E.: Neural message passing for quantum chemistry. In: International Conference on Machine Learning, pp. 1263–1272 (2017). PMLR
- [18] He, K., Zhang, X., Ren, S., Sun, J.: Deep residual learning for image recognition. In: Proceedings of the IEEE Conference on Computer Vision and Pattern Recognition, pp. 770–778 (2016)
- [19] Wu, Q., Diao, W., Dou, F., Sun, X., Zheng, X., Fu, K., Zhao, F.: Shape-based object extraction in high-resolution remote-sensing images using deep boltzmann machine. *International Journal of Remote Sensing* **37**(24), 6012–6022 (2016)
- [20] Microsoft: Microsoft/USBUILDINGFOOTPRINTS: Computer generated building footprints for the United States (2018). <https://github.com/microsoft/USBuildingFootprints>
- [21] Lin, G., Milan, A., Shen, C., Reid, I.: Refinenet: Multi-path refinement networks for high-resolution semantic segmentation. In: Proceedings of the IEEE Conference on Computer Vision and Pattern Recognition, pp. 1925–1934 (2017)

- [22] Xu, Y., Chen, Z., Xie, Z., Wu, L.: Quality assessment of building footprint data using a deep autoencoder network. *International Journal of Geographical Information Science* **31**(10), 1929–1951 (2017)
- [23] OpenStreetMap contributors: Planet dump retrieved from <https://planet.osm.org> . <https://www.openstreetmap.org> (2017)
- [24] Lopes, R.G., Ha, D., Eck, D., Shlens, J.: A learned representation for scalable vector graphics. In: *Proceedings of the IEEE/CVF International Conference on Computer Vision*, pp. 7930–7939 (2019)
- [25] Mino, A., Spanakis, G.: Logan: Generating logos with a generative adversarial neural network conditioned on color. In: *2018 17th IEEE International Conference on Machine Learning and Applications (ICMLA)*, pp. 965–970 (2018). IEEE
- [26] Sage, A., Agustsson, E., Timofte, R., Van Gool, L.: Logo synthesis and manipulation with clustered generative adversarial networks. In: *Proceedings of the IEEE Conference on Computer Vision and Pattern Recognition*, pp. 5879–5888 (2018)
- [27] Radford, A., Metz, L., Chintala, S.: Unsupervised representation learning with deep convolutional generative adversarial networks. In: Bengio, Y., LeCun, Y. (eds.) *4th International Conference on Learning Representations, ICLR 2016, San Juan, Puerto Rico, May 2-4, 2016, Conference Track Proceedings* (2016). <http://arxiv.org/abs/1511.06434>
- [28] Odena, A., Olah, C., Shlens, J.: Conditional image synthesis with auxiliary classifier gans. In: *International Conference on Machine Learning*, pp. 2642–2651 (2017). PMLR
- [29] Ha, D., Eck, D.: A neural representation of sketch drawings. In: *International Conference on Learning Representations* (2018)
- [30] Carlier, A., Danelljan, M., Alahi, A., Timofte, R.: Deepsvg: A hierarchical generative network for vector graphics animation. *Advances in Neural Information Processing Systems* **33**, 16351–16361 (2020)
- [31] Vaswani, A., Shazeer, N., Parmar, N., Uszkoreit, J., Jones, L., Gomez, A.N., Kaiser, Ł., Polosukhin, I.: Attention is all you need. *Advances in neural information processing systems* **30** (2017)
- [32] Bruna, J., Zaremba, W., Szlam, A., LeCun, Y.: Spectral networks and locally connected networks on graphs. In: *ICLR* (2014)
- [33] Defferrard, M., Bresson, X., Vandergheynst, P.: Convolutional neural networks on graphs with fast localized spectral filtering. *Advances in neural information processing systems* **29** (2016)



- [34] Velickovic, P., Cucurull, G., Casanova, A., Romero, A., Lio, P., Bengio, Y., *et al.*: Graph attention networks. *stat* **1050**(20), 10–48550 (2017)
- [35] Liu, C., Hu, Y., Li, Z., Xu, J., Han, Z., Guo, J.: Triangleconv: A deep point convolutional network for recognizing building shapes in map space. *ISPRS International Journal of Geo-Information* **10**(10), 687 (2021)
- [36] Wang, Y., Sun, Y., Liu, Z., Sarma, S.E., Bronstein, M.M., Solomon, J.M.: Dynamic graph cnn for learning on point clouds. *Acm Transactions On Graphics (tog)* **38**(5), 1–12 (2019)
- [37] Tailor, S.A., Jong, R., Azevedo, T., Mattina, M., Maji, P.: Towards efficient point cloud graph neural networks through architectural simplification. In: *Proceedings of the IEEE/CVF International Conference on Computer Vision*, pp. 2095–2104 (2021)
- [38] OpenGeospatialConsortium: OpenGIS Simple Features Specification For SQL. OpenGeospatialConsortium (2003). <http://www.opengis.org/>
- [39] Battaglia, P.W., Hamrick, J.B., Bapst, V., Sanchez-Gonzalez, A., Zambaldi, V., Malinowski, M., Tacchetti, A., Raposo, D., Santoro, A., Faulkner, R., *et al.*: Relational inductive biases, deep learning, and graph networks. *arXiv preprint arXiv:1806.01261* (2018)
- [40] Google Google (2010). <https://fonts.google.com/>
- [41] Duckham, M., Kulik, L., Worboys, M., Galton, A.: Efficient generation of simple polygons for characterizing the shape of a set of points in the plane. *Pattern recognition* **41**(10), 3224–3236 (2008)
- [42] Yan, X., Ai, T., Zhang, X.: Template matching and simplification method for building features based on shape cognition. *ISPRS International Journal of Geo-Information* **6**(8), 250 (2017)
- [43] Douglas, D.H., Peucker, T.K.: Algorithms for the reduction of the number of points required to represent a digitized line or its caricature. *Cartographica: the international journal for geographic information and geovisualization* **10**(2), 112–122 (1973)
- [44] Zhang, Z., Sabuncu, M.: Generalized cross entropy loss for training deep neural networks with noisy labels. *Advances in neural information processing systems* **31** (2018)
- [45] Kingma, D.P., Ba, J.: Adam: A method for stochastic optimization. In: *ICLR (Poster)* (2015)